Hydrodynamic Fingering Instability Induced by a Precipitation Reaction

Y. Nagatsu,[1,2] Y. Ishii,[2] Y. Tada,[2] and A. De Wit[3]
[1]Department of Chemical Engineering, Tokyo University of Agriculture and Technology, 2-24-16 Naka-cho, Koganei, Tokyo 184-8588, Japan
[2]Department of Materials Science and Engineering, Graduate School of Engineering, Nagoya Institute of Technology, Gokiso-cho, Showa-ku, Nagoya, Aichi 466-8555, Japan
[3]Nonlinear Physical Chemistry Unit, Faculté des Sciences, Université Libre de Bruxelles (ULB), CP231, 1050 Brussels, Belgium
(Received 31 July 2013; published 7 July 2014)

We experimentally demonstrate that a precipitation reaction at the miscible interface between two reactive solutions can trigger a hydrodynamic instability due to the buildup of a locally adverse mobility gradient related to a decrease in permeability. The precipitate results from an $A + B \rightarrow C$ type of reaction when a solution containing one of the reactants is injected into a solution of the other reactant in a porous medium or a Hele-Shaw cell. Fingerlike precipitation patterns are observed upon displacement, the properties of which depend on whether A displaces B or vice versa. A mathematical modeling of the underlying mobility profile confirms that the instability originates from a local decrease in mobility driven by the localized precipitation. Nonlinear simulations of the related reaction-diffusion-convection model reproduce the properties of the instability observed experimentally. In particular, the simulations suggest that differences in diffusivity between A and B may contribute to the asymmetric characteristics of the fingering precipitation patterns.

DOI: 10.1103/PhysRevLett.113.024502 PACS numbers: 47.55.P–, 47.15.gp, 47.56.+r, 47.70.Fw

Chemical reactions are able to influence and even more strikingly induce hydrodynamic fingering instabilities of a frontal interface when a high mobility fluid displaces a less mobile one in a porous medium. This occurs in viscous fingering if a less viscous fluid displaces a more viscous one [1]. Fingering can also result from a change in permeability in a porous medium as in reactive dissolution instabilities [2–10]. In these cases, the invading fluid contains chemicals which dissolve the solid matrix of the porous medium, leading to a related increase in porosity behind the reaction front. As a result, the resistance to flow decreases in these higher mobility reactive zones, which favors further dissolution, giving, thus, a positive feedback leading to instability. Dispersion of reactants is the stabilizing factor counteracting the growth of fluid channels in order to provide a fingered pattern with a given characteristic wavelength [2,5,7,10]. The reverse case of precipitation is not expected to destabilize an interface as the related decrease in permeability and, hence, in mobility behind the front is expected to block the flow rather than destabilize it. There is, however, increased interest to understand the effect of precipitation reactions during flow displacements in porous media in the context of CO_2 sequestration techniques [11–14]. Mineralization by which CO_2 injected in a porous medium could undergo precipitation reactions (to yield carbonates, for instance [13–16]) is indeed promising in view of a permanent safe storage of CO_2 in geological strata. Understanding the conditions in which precipitations can affect the stability of the spreading CO_2 plumes [12] is, thus, particularly important.

In this context, we demonstrate experimentally and explain theoretically how a precipitation reaction localized at the interface between two reactive solutions can trigger fingering patterns in a porous medium or in a Hele-Shaw cell. We develop a reaction-diffusion-convection (RDC) model coupling the evolution equation of the velocity field to a simple $A + B \rightarrow C$ reaction where A and B are solutes contained in the injected and displaced fluid while C is a precipitate. The mobility of the fluid inside the porous medium is modeled to decrease with the concentration of the precipitate. We show that the local production of the solid phase C in the reactive zone decreases locally the permeability and, hence, the mobility. A fingering instability develops in the region where a negative gradient of mobility is encountered along the direction of the flow. This precipitation mechanism of instability is asymmetric as the characteristics of the pattern depend on whether A is injected into B or vice versa. We explain that differences in the diffusion coefficients of the reactants can contribute to this asymmetry. We discuss the analogy of this local precipitation-induced fingering with classical viscous fingering and other reactive fingering instabilities.

The experimental setup is a horizontal Hele-Shaw cell which consists in two parallel glass plates separated by a thin gap [17,18]. The cell is initially filled with a solution of B. At time $t = 0$, a miscible solution of A is injected radially from a hole located in the center of the cell at a constant flow rate. The reverse case (B injected into A) is also performed. In the absence of reaction, both solutions of A and B have the same viscosity as that of water and similar densities so that

no hydrodynamic instability is observed, and the miscible interface expands as a circle. We investigate here how a simple $A + B \rightarrow C$ type of chemical reaction for which the product C is a solid precipitate can induce an instability of this interface. We use the following precipitation reaction:

$$Fe^{3+} + K_4[Fe(CN)_6] \rightarrow 3K^+ + KFe[Fe(CN)_6]. \quad (1)$$

The product $KFe[Fe(CN)_6]$ is a blue precipitate as seen in Figs. 1(c)–1(f). Another $A + B \rightarrow C$ reaction with no precipitate is studied in parallel as the reference case with no permeability change,

$$Fe^{3+} + SCN^- \rightarrow [Fe(SCN)]^{2+}, \quad (2)$$

where $[Fe(SCN)]^{2+}$ is a red ion in solution in the solvent [Figs. 1(a) and 1(b)]. Both reactions are very fast and can be treated as instantaneous. The dynamics in the reactive zone and the possible fingering pattern are followed by the color change induced by the reaction, all reactants being colorless. These reactions are the same as in our previous study of the effects of a precipitation reaction on viscous fingering when the solution of A is less viscous than the displaced solution of B [18]. The difference is that both reactants' solutions have here the same viscosity, so the instability can only be induced by the reaction.

Figure 1 shows the results of four different types of reactive displacement experiments for reaction (1) with precipitation and reaction (2) with no precipitation. For both reactions, we consider situations where the Fe^{3+} solution is either the displacing (case α) or the displaced (case β) solution, respectively. In the absence of precipitate

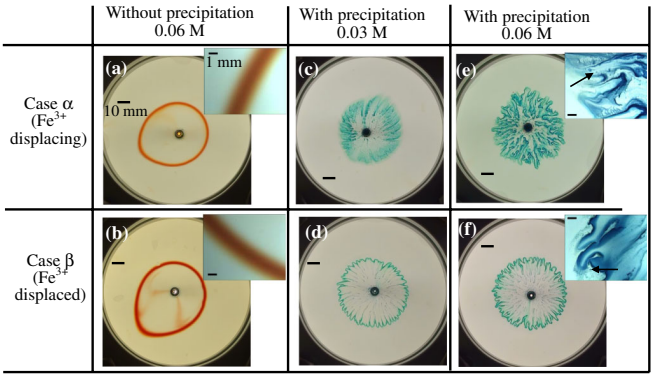

FIG. 1 (color online). Reactive displacement patterns without (a),(b) and with (c)–(f) precipitation at $t = 840$ s in a Hele-Shaw cell of gap $a = 0.2$ mm and with a flow rate $Q = 6.47 \times 10^{-10}$ m^3/s. The reactant concentration is either 0.03 M (c),(d) or 0.06 M (a),(b),(e),(f). α, β stand for the Fe^{3+} solution displacing and being displaced, respectively. Scale bars are 10 mm long. Inserts show a microscopic picture of the front taken by a digital microscope (FS1400, Nakaden, Japan) with 1 mm long scale bars and arrows indicating a typical size of the precipitation crystal.

[Figs. 1(a) and 1(b)], no fingering is observed, and the red product area expands radially in the course of time without fingered deformation for both cases α and β. On the contrary, in the presence of a precipitate, a fingering pattern is observed in all cases, i.e., for different concentrations tested and whether Fe^{3+} is injected [Figs. 1(c) and 1(e)] or displaced [Figs. 1(d) and 1(f)]. Microscopic pictures (inserts in Fig. 1) show that the product is a solution in the absence of precipitation and that, in the case of precipitation, the size of the solid crystals is much smaller than the typical size of the fingering pattern. This indicates that the fingering instability in Figs. 1(e) and 1(f) is not related to a dendritic growth of the solid phase but that the precipitation reaction is the motor of the hydrodynamic instability.

An analysis of Figs. 1(c)–1(f) shows that fingering is more concentrated and spreads over a broader area at larger concentrations and that the pattern is quite different in cases α and β. If Fe^{3+} is the displacing solution (case α), the blue precipitate is present in the whole zone behind the displacement front and, as seen in the movie of the Supplemental Material [19], this solid phase remains immobile once deposited. On the other hand, in case β, where Fe^{3+} is the displaced solution, the blue precipitate is located mainly within the reaction zone, and the fingered precipitate perimeter expands radially during the displacement (see the movie in the Supplemental Material [19]).

The fingering induced here by precipitation features an asymmetry, i.e., different characteristics whether A is injected into B or vice versa. This asymmetry does not exist in the stable case without precipitation, as expected [Figs. 1(a) and 1(b)]. Such asymmetries in reaction-induced fingering have already been reported in viscous fingering instabilities of reactive interfaces [20,21]. Simulations have shown that, in miscible systems, the asymmetry can be caused by a difference in diffusivity between the two reactants [21]. Here, the product is a solid, so the situation is different. We note, however, that the molecular weight of Fe^{3+} and that of $K_4[Fe(CN)_6]$ is 56 and 368, respectively. Thus, we can consider that the lighter ferric ion has a larger diffusion coefficient.

To clarify the mechanism at the origin of the hydrodynamic instability induced by the local precipitation reaction and test whether differences in diffusivity are important in the present dynamics, we next turn to a RDC model of the problem. We consider a simple $A + B \rightarrow C$ reaction where A and B are the reactants in miscible liquid solutions in equal initial concentration a_0 and same constant viscosity μ, while C is a solid product formed in the reaction zone upon displacement of one reactant solution by the other one. We analyze a two-dimensional flow in a porous medium described by Darcy's law (3) where $\kappa(c)$ is the permeability, which is a decreasing function of the concentration c of the precipitate. We assume, indeed, that the precipitate, by its presence in the pores of the porous

matrix or between the plates of a Hele-Shaw cell, decreases the volume of the void space and, thus, decreases the permeability. Experimental data on the $\kappa(c)$ dependence are very challenging to obtain [22]. Hence, by analogy with modeling of rock dissolution [5] and of miscible viscous fingering in which the viscosity is taken to vary exponentially with the concentration of the viscosity controlling solute [1,21,23–26], the functional dependence of the permeability κ on c is taken as a simple exponential decay, i.e., $\kappa = \kappa_0 \exp[-2R_\kappa(c/a_0)]$, such that if $c = 0$, the dimensionless permeability equals κ_0. We introduce the value of the permeability when $c = a_0/2$ as κ_h. The key parameter of the problem is then $R_\kappa = \ln(\kappa_0/\kappa_h)$, i.e., the mobility ratio comparing the mobility $M_0 = \kappa_0/\mu$ in the absence of precipitation with the mobility $M_h = \kappa_h/\mu$ when $c = a_0/2$, i.e., when all the precipitate is formed. Thus, as R_κ increases, the effects of the precipitation become larger. Larger reactant concentrations a_0 correspond to a larger amount of precipitate c and hence to smaller κ_h or equivalently to larger R_κ. Note that similar results can be obtained with other $\kappa(c)$ functions [5], provided κ decreases here with c. The nondimensional equations, where permeability, pressure, diffusivity, and concentration are scaled by κ_0, $\mu D_c/\kappa_0$, D_c, and a_0, respectively, are

$$\nabla \underline{u} = 0, \qquad \nabla p = -\frac{1}{\kappa(c)}\underline{u}, \tag{3}$$

$$\frac{\partial A}{\partial t} + \underline{u}\nabla A = \delta_A \nabla^2 A - D_a AB, \tag{4}$$

$$\frac{\partial B}{\partial t} + \underline{u}\nabla B = \delta_B \nabla^2 B - D_a AB, \tag{5}$$

$$\frac{\partial C}{\partial t} + \underline{u}\nabla C = \nabla^2 C + D_a AB, \tag{6}$$

$$\kappa = \exp(-2R_\kappa C), \tag{7}$$

where $D_a = ka_0 D_c/U^2$ is the Damköhler number, (A, B, C) are the dimensionless concentrations of species A, B, and C, and $\delta_{A,B} = D_{A,B}/D_C$ are the ratios of diffusion coefficients [24,26]. Here, k is the kinetic constant of the reaction, and U the rectilinear injection speed.

In classical viscous fingering and rock dissolution problems, the instability arises because a more mobile fluid displaces a less mobile one in a porous medium, i.e., because the mobility $M = \kappa/\mu$ decreases in the direction of the flow x. In the present situation, the viscosity μ is constant, and the mobility decreases as κ decreases due to precipitation. Fingering, thus, cannot develop in a precipitation front but may appear locally in regions where $\partial M/\partial x < 0$. This occurs thanks to the nonmonotonic character of the mobility profile [20,21,24–27] developing if precipitation occurs only locally in the reactive zone between the two solutions.

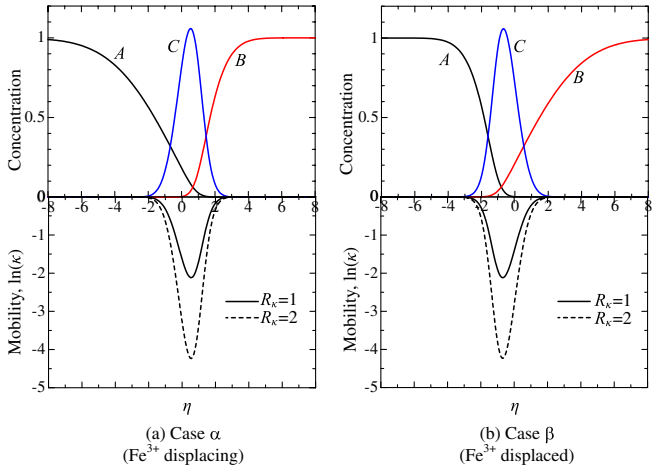

FIG. 2 (color online). Concentration and mobility profiles for $D_a = 1$. In (a) $\delta_A = 20$ and $\delta_B = 5$, while in (b) $\delta_A = 5$ and $\delta_B = 20$.

Figure 2 depicts the dimensionless concentration profiles of the various chemical species and of the mobility profile reconstructed using Eq. (7) on the basis of the product concentration profile. The horizontal axis is the dimensionless self-similar variable $\eta = x/\sqrt{4t}$, where t is the dimensionless time. We see that the mobility is constant and equal to 0 in the region of pure reactant A and B liquid solutions, while it is decreasing locally in the reactive zone where the precipitate C is produced. Fingering, thus, arises because locally, at the back of the reaction zone, the reactant solution A displaces the solid product zone of lower mobility. By analogy to what is observed in the case of reactive miscible viscous fingering with production of nonmonotonic viscosity profiles [26,27], the fingers extend toward the invading fluid (Fig. 1) upon the buildup of a local minimum in mobility due here to a minimum in permeability. The amplitude of the minimum in mobility increases when R_κ increases (Fig. 2), which is achieved experimentally when the concentration a_0 of the reactant solutions is increased. This is, again, coherent with the fact that more product is obtained at larger concentrations as seen in experiments (Fig. 1). The model, thus, shows that fingering can be triggered by a precipitation reaction thanks to a local decrease in permeability and, hence, of mobility along the direction of the flow.

To understand whether differences in diffusion coefficients can be the reason for the difference observed in the pattern depending on whether A displaces B or vice versa, we compare in Fig. 2 the mobility profiles for two cases, i.e., when $\delta_A = 20$ and $\delta_B = 5$ with the case $\delta_A = 5$ and $\delta_B = 20$. The former and latter cases correspond to cases α and β in the experiment, respectively. The precipitate C is logically considered as the species which diffuses the slowest. A corresponds to the fastest ferric ions and B to $K_4[Fe(CN)_6]$ in case α, and the reverse in case β. If the initial concentration and the diffusion coefficients of the

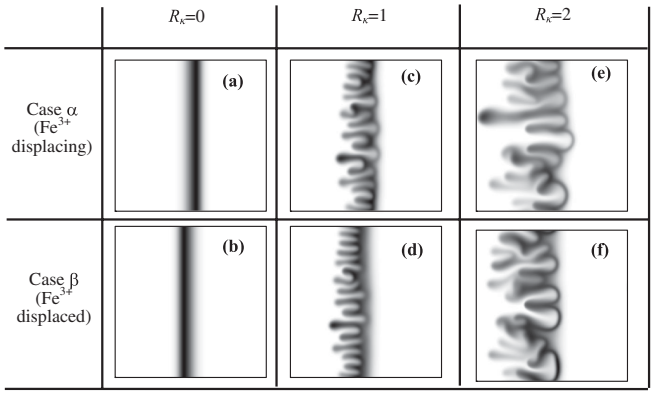

FIG. 3. Numerical nonlinear dynamics at $t = 800$, $D_a = 1$. In case α $\delta_A = 20$ and $\delta_B = 5$, while in case β $\delta_A = 5$ and $\delta_B = 20$. The injection is from left to right. Panels (a)–(f) of size 1020×1024 refer to the same conditions as in Fig. 1.

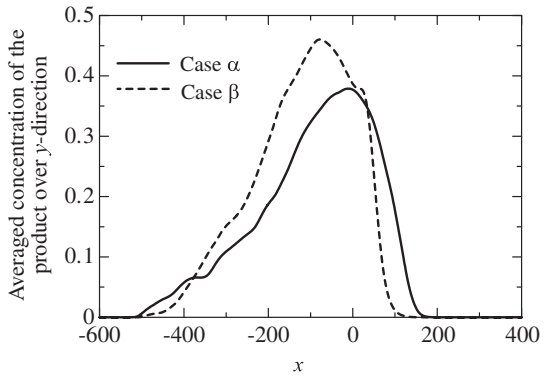

FIG. 4. Averaged concentration of the product over the y direction, when $R_k = 2$, $t = 800$, $D_a = 1$. In case α, $\delta_A = 20$ and $\delta_B = 5$, while in case β, $\delta_A = 5$ and $\delta_B = 20$. Here, $x = 0$ is the initial location of the interface between the displacing and displaced fluids, and the flow is directed toward positive x.

two reactants are the same, the concentration profiles are symmetric with regard to $\eta = 0$ [21,28]. When the diffusivity of the reactant initially included in the displacing solution is larger [case α, Fig. 2(a)], the negative mobility gradient is slightly different than in the reverse case where the faster diffusing reactant is in the displaced solution [case β, Fig. 2(b)]. To check the effect of this asymmetry even further, let us now turn to nonlinear simulations.

The governing equations (3)–(7) are numerically integrated by the pseudospectral method developed by Tan and Homsy [23] with periodic boundary conditions and an initial condition similar to those used in studies of reactive viscous fingering [21,26]. Figure 3 shows the numerical dynamics in four different cases depending on the diffusivity ratio and R_κ by displaying the product concentration field on a gray scale. First, the fingering instability is obtained in all cases involving precipitation with fingers extending backwards. The system remains stable when $R_\kappa = 0$, which confirms that double diffusive instabilities [29–31] are not operational in our precipitation case, as the A and B reactant solutions have here the same viscosity and density. A comparison between the upper and lower rows shows the effect of changing the ratio of diffusivity of the reactants with larger diffusivity initially in the displacing and displaced solutions, respectively, i.e., to cases α and β. We can qualitatively find that the product is more evenly distributed in case α, while it is more concentrated at the right forward invading front of the fingered zone in case β independent of R_κ. Moreover, the comparison between the left and right columns for $R_\kappa \neq 0$ shows that fingering is more pronounced at a given time when R_κ is larger. These results are in good agreement with the experimental ones.

From the nonlinear simulations, one can compute one-dimensional concentration profiles of the product C resulting from an average of the 2D field over the y direction (Fig. 4). This result is averaged over five runs with different initial noise. As shown in Fig. 4, the product is more concentrated at the fingertips in case β. This result is consistent with the experimental results, and, hence, nonlinear simulations show that the asymmetric properties observed in the experiments can be explained in terms of an asymmetry of diffusivity. This is probably not enough to explain the full dynamics, and additional effects should be taken into account in future studies like possible mechanical or non-Newtonian effects or local changes in viscosity (especially in case β where the solid is advected by the flow and there is, thus, locally a suspension of particles that most probably affects the viscosity). Nevertheless, the present model already shows that a change of mobility due to a localized decrease of permeability triggered by a reaction is able to trigger fingering and that the related RDC model correctly reproduces all features of the instability.

In conclusion, we have experimentally and theoretically studied hydrodynamic fingering triggered by a chemical precipitation reaction in the miscible contact zone between two liquid solutions of reactants in a porous medium or Hele-Shaw cell. We showed that fingering is due to a local decrease in mobility related to the reduction of the permeability due to the presence of the precipitate. The fingered pattern is asymmetric, i.e., different depending on whether A displaces B or vice versa, which could be due to differences in diffusivity between A and B. The experiments and nonlinear simulations of a RDC model give results in good agreement. We emphasize that the modeling of this precipitation-induced fingering is analogous to that of reactive viscous fingering [20,21,24–27] and dissolution-driven fingering [2–10] with nonmonotonic profiles. The present study paves the way to future detailed analysis of the influence of precipitation reactions on the stability of displacement processes in porous media. It explains, for instance, why local precipitation of carbonates [13,14], among others, might destabilize the flow during CO_2 injection processes at the heart of sequestration techniques.

We acknowledge JSPS KAKENHI Grant No. 22686020, Prodex, and FRS-FNRS under the PDR-FORECAST project for financial support. We are grateful to Professor S. Iwata, Nagoya Institute of Technology, for helpful discussions and to Ms. R. Tsuzuki, Tokyo University of Agriculture and Technology, for her help in the experiments using a digital microscope.

[1] G. M. Homsy, Annu. Rev. Fluid Mech. **19**, 271 (1987).
[2] J. Chadam, D. Hoff, E. Merino, P. Ortoleva, and A. Sen, IMA J. Appl. Math. **36**, 207 (1986).
[3] J. D. Sherwood, Chem. Eng. Sci. **42**, 1823 (1987).
[4] G. Daccord and R. Lenormand, Nature (London) **325**, 41 (1987).
[5] E. J. Hinch and B. S. Bhatt, J. Fluid Mech. **212**, 279 (1990).
[6] C. Wei and P. Ortoleva, Earth Sci. Rev. **29**, 183 (1990).
[7] S. Crompton and P. Grindrod, IMA J. Appl. Math. **57**, 29 (1996).
[8] F. Renard, J.-P. Gratier, P. Ortoleva, E. Brosse, and B. Bazin, Geophys. Res. Lett. **25**, 385 (1998).
[9] N. Kalia and V. Balakotaiah, Chem. Eng. Sci. **64**, 376 (2009).
[10] P. Szymzak and A. J. C. Ladd, Earth Planet. Sci. Lett. **301**, 424 (2011).
[11] J. Ennis-King and L. Paterson, Int. J. Greenhouse Gas Contr. **1**, 86 (2007).
[12] S. Berg and H. Ott, Int. J. Greenhouse Gas Contr. **11**, 188 (2012).
[13] O. Hammer, D. K. Dysthe, B. Lelu, H. Lund, P. Meakin, and B. Jamtveit, Geochim. Cosmochim. Acta **72**, 5009 (2008).
[14] C. Zhang, K. Dehoff, N. Hess, M. Oostrom, T. W. Wietsma, A. J. Valocchi, B. W. Fouke, and C. J. Werth, Environ. Sci. Technol. **44**, 7833 (2010).
[15] B. P. McGrail, H. T. Schaef, A. M. Ho, Y.-J. Chien, J. J. Dooley, and C. L. Davidson, J. Geophys. Res. **111**, B12201 (2006).
[16] A. R. White and T. Ward, Chaos **22**, 037114 (2012).
[17] Y. Nagatsu, K. Matsuda, Y. Kato, and Y. Tada, J. Fluid Mech. **571**, 475 (2007).
[18] Y. Nagatsu, S.-K. Bae, Y. Kato, and Y. Tada, Phys. Rev. E **77**, 067302 (2008).
[19] See the Supplemental Material at http://link.aps.org/supplemental/10.1103/PhysRevLett.113.024502 for movies of the precipitation dynamics accelerated 64×.
[20] T. Podgorski, M. C. Sostarecz, S. Zorman, and A. Belmonte, Phys. Rev. E **76**, 016202 (2007).
[21] T. Gérard and A. De Wit, Phys. Rev. E **79**, 016308 (2009).
[22] L. Luquot and P. Gouze, Chem. Geol. **265**, 148 (2009).
[23] C. T. Tan and G. M. Homsy, Phys. Fluids **31**, 1330 (1988).
[24] S. H. Hejazi, P. M. J. Trevelyan, J. Azaiez, and A. De Wit, J. Fluid Mech. **652**, 501 (2010).
[25] S. H. Hejazi and J. Azaiez, Chem. Eng. Sci. **65**, 938 (2010).
[26] Y. Nagatsu and A. De Wit, Phys. Fluids **23**, 043103 (2011).
[27] L. A. Riolfo, Y. Nagatsu, S. Iwata, R. Maes, P. M. J. Trevelyan, and A. De Wit, Phys. Rev. E **85**, 015304(R) (2012).
[28] L. Gálfi and Z. Rácz, Phys. Rev. A **38**, 3151 (1988).
[29] S. E. Pringle, R. J. Glass, and C. A. Cooper, Transp. Porous Media **47**, 195 (2002).
[30] M. Mishra, P. M. J. Trevelyan, C. Almarcha, and A. De Wit, Phys. Rev. Lett. **105**, 204501 (2010).
[31] L. Lemaigre, M. A. Budroni, L. A. Riolfo, P. Grosfils, and A. De Wit, Phys. Fluids **25**, 014103 (2013).